

Accepted Manuscript

A high signal-to-background ratio H₂S-specific fluorescent probe based on nucleophilic substitution and its bioimaging for generation H₂S induced by Ca²⁺ in vivo

Jin Kang, Fangjun Huo, Yishan Yao, Caixia Yin

PII: S0143-7208(19)31172-6

DOI: <https://doi.org/10.1016/j.dyepig.2019.107755>

Article Number: 107755

Reference: DYPI 107755

To appear in: *Dyes and Pigments*

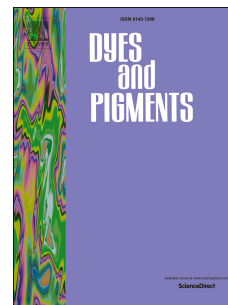
Received Date: 22 May 2019

Revised Date: 17 July 2019

Accepted Date: 25 July 2019

Please cite this article as: Kang J, Huo F, Yao Y, Yin C, A high signal-to-background ratio H₂S-specific fluorescent probe based on nucleophilic substitution and its bioimaging for generation H₂S induced by Ca²⁺ in vivo, *Dyes and Pigments* (2019), doi: <https://doi.org/10.1016/j.dyepig.2019.107755>.

This is a PDF file of an unedited manuscript that has been accepted for publication. As a service to our customers we are providing this early version of the manuscript. The manuscript will undergo copyediting, typesetting, and review of the resulting proof before it is published in its final form. Please note that during the production process errors may be discovered which could affect the content, and all legal disclaimers that apply to the journal pertain.



Highlights

1
2
3
4
5
6
7
8
9
10
11
12
13
14
15
16
17
18
19
20
21
22
23
24
25
26
27
28
29

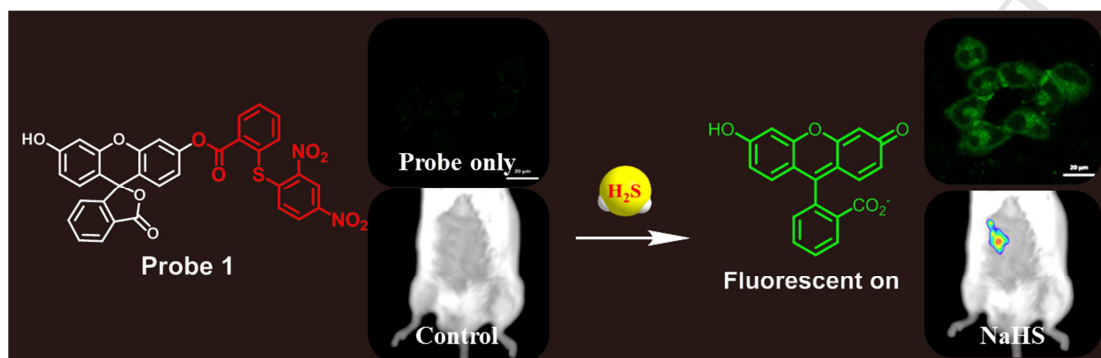
1. This probe exhibit high signal-to-background ratio in response to H₂S.
2. This probe was used to detect endogenous generation H₂S induced by Ca²⁺ mediated cystathionine γ -lyase (CSE).
3. This probe was successfully used to detect exogenous hydrogen sulfide in mice.

30

31

Abstract Graphic

32 The statement:



33

34 A novel fluorescence H₂S probe based on nucleophilic substitution reactions, which
35 with high signal-to-background ratios. This probe was successfully used to imaging
36 ex-/endogenous H₂S in living cells, and exogenous H₂S in mice.

37

38

39

40

41

42

43

44

45

46

47

48

49

50

51

52 **A high signal-to-background ratio H₂S-specific fluorescent probe**
53 **based on nucleophilic substitution and its bioimaging for generation**
54 **H₂S induced by Ca²⁺ in vivo**

55 Jin Kang,^{1a} Fangjun Huo,^{1b} Yishan Yao,^{1c} Caixia Yin^{a,*}

56 ^a *Institute of Molecular Science, Key Laboratory of Materials for Energy Conversion*
57 *and Storage of Shanxi Province, Shanxi University, Taiyuan 030006,*

58 ^b *Research Institute of Applied Chemistry, Shanxi University, Taiyuan, 030006, China.*

59 ^c *State Key Laboratory of Toxicology and Medical Countermeasures, Beijing Institute*
60 *of pharmacology and Toxicology, No.27 Taiping Road, Haidian District,*
61 *Beijing, 100850, P. R. China.*

62 *Corresponding author: C.X. Yin, E-mail: yincx@sxu.edu.cn, Tel/Fax:
63 +86-351-7011022.

64 **Abstract** Hydrogen sulfide (H₂S), a new endothelium-derived relaxing factor
65 (EDRF), which plays vital roles in regulating intracellular redoxstatus and other
66 fundamental signaling processes involved in human health and disease. In this work,
67 we designed a fluorescent probe for H₂S successive nucleophilic reaction with high
68 signal-to-background (S/B) ratio. In the probe, we utilized 2-mercaptobenzoic acid as
69 the distinguish reaction site and introduced 2,4-dinitrophenyl to provide appropriate
70 steric hindrance to realize specific response on well-structured H₂S. Other substances
71 sulfur-containing do not disturb the detection of H₂S. The max emission with 197-fold
72 enhancement exhibits high signal-to-background ratio. The detection limit was
73 calculated to be 64 nM. Imaging assays in living cells showed that the probe could
74 penetrate cells membrane easily and allowed to detect endogenous generation H₂S
75 induced by Ca²⁺ mediated cystathionine γ -lyase (CSE). Moreover, the probe was
76 successfully used to detect exogenous H₂S in mice.

77 **Keywords:** H₂S-specific; Two nucleophilic; Ca²⁺ mediated; Vivo

78

79

80 1. Intruduction

81 H₂S is extensively exist in a wide variety of industries such as oil exploitation,
82 natural gas well, tunnel and sewage disposal [1-4]. Exposure to high level H₂S
83 atmosphere may cause respiratory symptoms, cardiovascular abnormalities and
84 neurological disorders [5-7]. H₂S was found as the third multifunctional
85 gasotransmitter along with nitric oxide (NO) and carbon monoxide (CO) since last
86 decades [8-10]. H₂S influences a wide range of physiological and pathophysiological
87 processes, including its ability to act as a neurotransmitter [11], regulator of blood
88 pressure [12], immunomodulator [13] or anti-apoptotic agent [14], together with its
89 great pharmacological potential, such as cardioprotection [15], endogenous
90 stimulation of angiogenesis [16] and mitochondrial bioenergetics [17]. However,
91 abnormally H₂S concentrations have been significant associated with alzheimer's
92 disease, down's syndrome, diabetes and liver cirrhosis [18-21]. Physiological effects
93 of H₂S are concentration-dependent, thus, in order to benefit from H₂S, the
94 concentration of H₂S must be maintained at the appropriate level. In mammals,
95 endogenous H₂S is synthesized naturally by several enzymes, including cystathionine
96 γ -lyase (CSE), cystathionine β -synthetase (CBS) and 3-mercaptopyruvate
97 sulfurtransferase (MST)/cysteine aminotransferase (CAT) [22-25]. Yang et al. reported
98 that the activity of cystathionine γ -lyase (CSE), an important enzyme responsible for
99 H₂S physiological generation in animals, could be activated by calcium-calmodulin
100 pathway [26]. However, the mechanism of Ca²⁺ induced intracellular H₂S production
101 in living cells has not been elucidated. Therefore, developing selective and sensitive

102 detection tools for H₂S in complex biological systems is important.

103 Traditional methods of H₂S detection, including methylene blue method [27], lead
104 acetate [28], electrochemical sensors [29], gas chromatography [30] and
105 monobromobimane derivatization are often limited by poor compatibility with
106 biosystem, limited temporal resolution or rigorous preparation requirements [31-32].
107 In contrast, fluorescent probes with highly sensitive, selective, nondestructive are
108 suitable for detection of this volatile, gaseous molecule with readily available
109 instruments [33-36]. In the past several years, a number of fluorescent probes for H₂S
110 have been reported [37-41]. However, probes with high signal-to-background (S/B)
111 ratio are rare. In bio-imaging, the probe with high S/B ratio is benefit for obtaining
112 more accurate and reliable signals. There are two ways to improve the probe's S/B
113 ratio: (1) Increase extent of fluorescence enhancement; (2) Improve selectivity.
114 Moreover, the application of fluorescent probes to the H₂S signaling pathway is still
115 rare.

116 The 2,4-dinitrophenyl (DNP) ether moiety has been employed extensively as a
117 protecting group for tyrosines in peptide synthesis [42]. Direct assemble the DNP
118 group onto various kinds of fluorophores have yielded a series H₂S probes [43-47].
119 Indeed, biothiols can also remove DNP group, the selectivity of these probes are
120 unsatisfactory [48-49]. In this work, we employed the DNP derivative
121 2-((2,4-dinitrophenyl)thio)benzoic acid as the masking group link to the fluorescein
122 and obtained the probe (**Probe 1**) (Scheme 1). The probe exhibits high selectivity and
123 significant fluorescence enhancement up to 197-fold upon the detection of H₂S.

124 Furthermore, Ca^{2+} induced H_2S production in HeLa cells was directly visual
125 demonstration use the probe.

126 2. Preparation and characterization of compounds

127 2.1. Preparation of **Probe 1**.

128 The **Probe 1** was synthesized from the compound 1 via an ester moiety link to
129 fluorescein (Scheme 1). The compound 1 was synthesized use the same methods as
130 previous literature [50].

131 <Inserted Scheme 1>

132 Compound 1 (1.0 mmol, 0.32 g) and fluorescein (1.0 mmol, 0.33 g) were dissolved
133 into 25 mL dichloromethane, added N-(3-dimethylaminopropyl)-N-ethyl carbodi
134 imide hydrochloride (EDC) (1.0 mmol, 0.19 g) and 4-dimethylaminopyridine (DMAP)
135 (0.10 mmol, 0.01 g). Surrounded by Ar, the reactant stired overnight (r.t.). Then
136 solvent was evaporated and resulted residue was subjected to column chromatography.
137 Probe was obtained as a yellow powder (0.19 g, yield: 30 %).

138 2.2. Characterization of **Probe 1**

139 ^1H NMR (600 MHz, $\text{DMSO-}d_6$) δ 8.88 (d, $J = 2.5$ Hz, 1H), 8.34 (t, $J = 8.0$ Hz, 3H),
140 8.05 (d, $J = 7.6$ Hz, 1H), 7.85 (d, $J = 5.7$ Hz, 4H), 7.80 (t, $J = 7.5$ Hz, 1H), 7.75 (t, $J =$
141 7.3 Hz, 1H), 7.37-7.34 (m, 2H), 7.15 (d, $J = 9.0$ Hz, 2H), 6.96 (d, $J = 8.7$ Hz, 2H),
142 6.91 (d, $J = 8.7$ Hz, 2H). ^{13}C NMR (150 MHz, $\text{DMSO-}d_6$) δ 163.4, 151.5, 150.6,
143 144.9, 144.4, 144.3, 137.5, 134.4, 133.5, 132.1, 131.3, 130.2, 129.9, 129.3, 127.6,
144 124.9, 123.9, 121.0, 118.3, 116.5, 110.3. ESI-MS m/z : [probe + H] $^+$ Calcd for
145 635.07604, Found 635.07525; [probe + Na] $^+$ Calcd for 657.05804, Found 657.05683.

146 3. Results and Discussion

147 3.1 Spectra properties of **Probe 1** response to H_2S .

148 Firstly, we evaluated the UV-vis spectra properties of **Probe 1**. As shown in Fig. 1,
149 in 2 mL DMSO : PBS (v/v, 7 : 3, pH = 7.4) solution of **Probe 1** (25 μ M), gradually
150 added HS^- (0-300 μ M), the absorbance at 338 nm increased with concomitant
151 appearance of absorbance at 475 nm in a short time frame (10 min). Similarly, we also
152 studied the reaction between **Probe 1** and biothiols (Cys, Hcy and GSH) in UV-vis
153 spectrometer (Fig. S6 a, b, c). Under the same conditions, the addition of Cys (500
154 μ M) caused a neglectable absorbance enhancement at 338 nm, and Hcy (500
155 μ M)/GSH (500 μ M) couldn't cause obvious changes in UV-vis spectra.

156 <Inserted Figure 1>

157 The **Probe 1** is considered to be a high S/B ratio probe. On the one hand, high S/B
158 ratio probe depend on the extent of fluorescence enhancement. As predicted, the
159 incremental addition of HS^- (0-70 μ M) to the solution DMSO : PBS (v/v, 7 : 3, pH =
160 7.4) of **Probe 1** (5 μ M) resulted in a dramatic enhancement of the emitting band
161 centered at 538 nm in 10 min (Fig. 2a). Finally, the max emission has 197-fold
162 enhancement. On the other hand, the high selectivity is very important condition for
163 high S/B ratio probe. The **Probe 1** was treated with HS^- and various relevant analyte
164 (100 eq.) in DMSO : PBS (v/v, 7 : 3, pH = 7.4). As shown in Fig. 2b, the **Probe 1** was
165 highly selective for HS^- versus biological relevant thiols or HSO_3^- . These results
166 demonstrate the excellent selectivity of the probe to H_2S . These above experiment
167 results, the emission of **Probe 1** has a large enhancement (197-fold) and the high

168 selective of the **Probe 1** fulfilled the requirements of high S/B ratio probe. Hence, the
169 probe is a H₂S-specific fluorescent probe with high S/B ratio.

170 <Inserted Figure 2>

171 3.2 Working curve and time dependents

172 Furthermore, a plot of fluorescent intensities at 538 nm versus the concentrations of
173 H₂S showed a good linearity ($R^2 = 0.991$): $F - F_0 = 94.24c - 293.60$ (Fig. 3a). With the
174 definition: Detection limit = $3\sigma/k$, the detection limit evaluated as 64 nM. In order to
175 evaluate the response speed of **Probe 1** towards H₂S, we examined the reactivity of
176 probe (5 μ M) towards the HS⁻ (10 eq.) through time-dependent fluorescence
177 spectroscopy in DMSO : PBS (v/v, 7 : 3, pH = 7.4). As the Fig. 3b depicted, the
178 reaction could be completed within 10 min.

179 <Inserted Figure 3>

180 3.3. Proposed mechanism

181 The proposed mechanism of **Probe 1** was depicted in the Scheme 2. The H₂S
182 nucleophilic substitution the carbonyl group of **Probe 1**, result in the protect group
183 cleaved and released the fluorescein and compound 2 [51]. Furthermore, the
184 mechanism was proved by the ESI-MS spectra analysis (Fig. S9). ESI-MS of a
185 solution mixture of **Probe 1** and NaHS exhibited m/z peaks at 331.0611, 198.9816 in
186 accordance with the fluorescein and compound 2 respectively.

187 <Inserted Scheme 2>

188 3.4 Cytotoxicity experiments

189 HepG2 cells were cultured in 96-well plates. The cell number was determined and a

190 serial dilution on **Probe 1** was performed in culture medium (without serum),
191 incubated for 5 or 10 h. Subsequently, CCK-8 (10 % in serum free culture medium)
192 was added to each well, which was washed with PBS two times and the plate was
193 incubated for another 1 h. Then measure optical densities at 450 nm. Cytotoxicity
194 assay demonstrating the **Probe 1** was benign to cells and has the potential to be used
195 in biological applications (Fig. S8).

196 3.5. Imaging of living cells

197 The HepG2 cells incubated with **Probe 1** (5 μM) only for 20 min showed no
198 fluorescence in the green channel (Fig. 4 a1). In contrast, treatment of **Probe 1**-loaded
199 cells with 20 μM NaHS for 20 min triggered an obvious increased in green
200 fluorescence signal (Fig. 4 b1).

201 <Inserted Figure 4>

202 Encouraged by its good sensing performances for H_2S in vitro, we applied **Probe 1**
203 to image the endogenously generated H_2S by exogenous compound stimulation.
204 S-Nitroso-N-acetyl-DL-penicillamine (SNP) was used to stimulate the generation of
205 endogenous H_2S in HepG2 cells. As we expected, after incubation with 10 μM SNP
206 for 1 h, the fluorescence intensities from the green channel clearly increased, which
207 are similar to that of the addition of exogenous NaHS (Fig. 5 d1),. These results
208 indicated that **Probe 1** capable of visualization of endogenous H_2S generation in
209 HepG2 cells. These cell experiments showed the **Probe 1** can thus be used to imaging
210 ex/endogenous H_2S in living cells.

211 <Inserted Figure 5>

212 3.6. Imaging the Ca^{2+} -dependent H_2S

213 Ca^{2+} is the second messenger and involved in a variety of intracellular signaling
214 pathways. According to reported, that calcium-calmodulin regulating the activity of
215 cystathionine γ -lyase (CSE) responsible for H_2S physiological generation in animals.
216 To demonstrate the mechanism of Ca^{2+} induced intracellular H_2S production in cells,
217 we conducted imaging experiments with **Probe 1** in Hela cells under conditions of
218 both negative and positive controls. No fluorescent signal was observed in green
219 channel when the cells were pre-incubated with DL-propargylglycine (PAG, which
220 suppresses CSE) along with **Probe 1** and Ca^{2+} . In contrast, obvious fluorescent was
221 observed when the cells were pre-incubated with Ca^{2+} and **Probe 1**, or cells
222 pre-incubated with aminooxyacetic acid (AOAA, a potent inhibitor of CBS) along
223 with **Probe 1** and Ca^{2+} . This indicated that CSE contributes to the observed H_2S
224 generation upon Ca^{2+} stimulation.

225 <Inserted Figure 6>

226 3.7. Imaging of living mice

227 Furthermore, we applied **Probe 1** imaging in mice. The Kunming mice were fed
228 commercial mouse chow in individual cages and left to freely wander in their housing
229 for two weeks with 12 h dark/light cycles for acclimatization before the experiment. A
230 living animal imaging system is used in imaging the mice. After all the preparatory
231 work was completed, the mice were under anesthesia with 100 mL pentobarbital
232 intraperitoneal injection. As Fig. 7 shows, the mice were injected with 50 mM of

233 **Probe 1** in the abdomen, HS^- was carefully injected into the same location. Then, the
234 fluorescence images were recorded at different periods of time (0, 5, 10, 15 min).
235 These results displayed that **Probe 1** could visualize the endogenous H_2S in vivo.

236 <Inserted Figure 7>

237 **4. Conclusions**

238 In conclusion, we prepared a fluorescein-based H_2S -specific probe **Probe 1** with
239 high S/B ratio. The results of UV-vis spectrum and fluorescence emission spectrum
240 studies showed that **Probe 1** had good selectivity for H_2S and having a 64 nM
241 detection limit for H_2S . Kinetics studies showed that the response can be completed in
242 10 min. Furthermore, this probe was used to directly image Ca^{2+} -dependent H_2S
243 production, and in vivo imaging.

244 **5. Acknowledgments**

245 We thank the National Natural Science Foundation of China (No. 21775096,
246 21302223), Shanxi Province "1331 project" key innovation team construction plan
247 cultivation team (2018-CT-1), Shanxi Province Foundation for Returnees (2017-026),
248 Shanxi Province Science Foundation for Youths (201701D221061), Scientific
249 Instrument Center of Shanxi University (201512).

250

251

252

253

254

255 **References**

- 256 [1] Haggard HW. The toxicity of hydrogen sulphide. *J. Ind. Hyg. Toxicol*
257 1925;7:113-121.
- 258 [2] Poda GA. Hydrogen sulfide can be handled safely. *Arch. Environ. Health*
259 1966;12:795-800.
- 260 [3] Yant WP. Hydrogen sulphide in industry-occurrence, effects, and treatment. *Am. J.*
261 *Public Health Nations Health* 1930;20:598-608.
- 262 [4] Qian Y, Karpus J, Kabil O, Zhang SY, Zhu HL, Banerjee R, Zhao J, He C.
263 Selective fluorescent probes for live-cell monitoring of sulphide. *Nat. Commun*
264 2011;2:495.
- 265 [5] Wang X, Sun J, Zhang WH, Ma XX, Lv JZ, Tang B. A near-infrared ratiometric
266 fluorescent probe for rapid and highly sensitive imaging of endogenous hydrogen
267 sulfide in living cells. *Chem. Sci* 2013;4:2551-2556.
- 268 [6] Liu CR, Pan J, Li S, Zhao Y, Wu LY, Berkman CE, Whorton AR, Xian M.
269 Capture and visualization of hydrogen sulfide by a fluorescent probe. *Angew.*
270 *Chem. Int. Ed* 2011; 50:10327-10329.
- 271 [7] Filipovic MR, Zivanovic J, Alvarez B, Banerjee R. Chemical biology of H₂S
272 signaling through persulfidation. *Chem. Rev* 2018;118:1253-1337.
- 273 [8] Abe K, Kimura H. The possible role of hydrogen sulfide as an endogenous
274 neuromodulator. *The J. Neurosci* 1996;16:1066-1071.

- 275 [9] Lin VS, Chen W, Xian M, Chang CJ. Chemical probes for molecular imaging
276 and detection of hydrogen sulfide and reactive sulfur species in biological
277 systems. *Chem. Soc. Rev* 2015;44:4596-4618.
- 278 [10] Eberhardt M, Dux M, Namer B, Filipovic MR. H₂S and NO cooperatively
279 regulate vascular tone by activating a neuroendocrine HNO-TRPA1-CGRP
280 signalling pathway. *Nat. Commun* 2014;5:4381.
- 281 [11] O'Sullivan SE. What is the significance of vascular hydrogen sulphide (H₂S)? *Brit.*
282 *J. Pharmacol* 2010;149:609-610.
- 283 [12] Perini R, Fiorucci S, Wallace JL. Mechanisms of nonsteroidal anti-inflammatory
284 drug-induced gastrointestinal injury and repair: a window of opportunity for
285 cyclooxygenase-inhibiting nitric oxide donors. *Can. J. Gastroenterol*
286 2004;18:229-236.
- 287 [13] Sodha NR, Clements RT, Feng J, Liu Y, Bianchi C, Horvath EM, Szabo C, Sellke
288 FW. The effects of therapeutic sulfide on myocardial apoptosis in response to
289 ischemia-reperfusion injury. *Eur. J. Cardio-Thorac* 2008;33:906-913.
- 290 [14] Lavu M, Bhushan S, Lefer DJ. Hydrogen sulfide-mediated cardioprotection:
291 mechanisms and therapeutic potential. *Clin. Sci* 2011;120:219-229.
- 292 [15] Bir SC, Kolluru GK, Fang K, Kevil CG. Redox balance dynamically regulates
293 vascular growth and remodeling. *Semin. Cell Dev. Biol* 2012;23:745-757.
- 294 [16] Kabil O, Banerjee R. Redox biochemistry of hydrogen sulfide. *J. Biol. Chem*

- 295 2010;285:21903-21907.
- 296 [17] Wu D, Si W, Wang M, Lv S, Ji A, Li Y. Hydrogen sulfide in cancer: friend or foe?
297 Nitric Oxide 2015;50:38-45.
- 298 [18] Fan K, Li N, Qi J, Yin P, Zhao C, Wang L, Li Z, Zha X. Wnt/beta-catenin
299 signaling induces the transcription of cystathionine- γ -lyase, a stimulator of tumor
300 in colon cancer. Cell Signal 2014;26:2801-2808.
- 301 [19] Altaany Z, Ju YJ, Yang GD, Wang R. The coordination of S-sulfhydration,
302 S-nitrosylation, and phosphorylation of endothelial nitric oxide synthase by
303 hydrogen sulfide. Sci. Signal 2014;7:87.
- 304 [20] Tai IH, Sheen JM, Lin YJ, Yu HR, Tiao MM, Chen CC, Huang LT, Tain YL.
305 Maternal N-acetylcysteine therapy regulates hydrogen sulfidegenerating pathway
306 and prevents programmed hypertension in male offspring exposed to prenatal
307 dexamethasone and postnatal high-fat diet. Nitric Oxide 2016;53:6-12.
- 308 [21] Wang R. Physiologicalimplications of hydrogen sulfide: a whiff exploration that
309 blossomed. Physiological Rev 2012;92:791-896.
- 310 [22] Li Q, Lancaster JR. Chemical foundations of hydrogen sulfide biology. Nitric
311 Oxide 2013;35:21-34.
- 312 [23] Kabil O, Zhou Y, Banerjee R. Human cystathionine- β -synthase is a target for
313 sumoylation. Biochem 2006;45:13528-13536.
- 314 [24] Yamanishi M, Kabil O, Sen S, Banerjee R. Structural insights into pathogenic

- 315 mutations in heme-dependent cystathionine- β -synthase. *J. Inorg. Biochem.*
316 2006;100:1988-1995.
- 317 [25] Yang GD, Wu LY, Jiang B, Yang W, Qi JS, Cao K, Meng QH, Mustafa AK, Mu
318 WT, Zhang SM, Snyder SH, Wang R. H₂S as a Physiologic Vasorelaxant:
319 Hypertension in Mice with Deletion of Cystathionine γ -Lyase. *Science*
320 2008;322:587-590.
- 321 [26] Wang MJ, Cai WJ, Zhu YC. Hydrogen sulphide in cardiovascular system: a
322 cascade from interaction between sulphur atoms and signalling molecules. *Life*
323 *Sci* 2016;153:188-197.
- 324 [27] Kuban V, Dasgupta PK, Marx JN, Nitroprusside and Methylene Blue Methods
325 for Silicone Membrane Differentiated Flow Injection Determination of Sulfide in
326 Water and Wastewater. *Anal. Chem* 1992;64:36-43.
- 327 [28] Wei Y, Kenyon C, Roles for ROS and Hydrogen Sulfide in the Longevity
328 Response to Germline Loss in *Caenorhabditis Elegans*. *Proc. Natl. Acad. Sci*
329 2016;113:E2832-E2841.
- 330 [29] Xu T, Scafa N, Xu LP, Zhou S, Abdullah Al-Ghanem K, Mahboob S, Fugetsu B,
331 Zhang X. Electrochemical hydrogen sulfide biosensors. *Analyst*
332 2016;141:1185-1195.
- 333 [30] Vitvitsky V, Banerjee R. H₂S analysis in biological samples using gas
334 chromatography with sulfur chemiluminescence detection. *Methods Enzymol*
335 2015;554:111-123.

- 336 [31] Ida T, Sawa T, Ihara H, Tsuchiya Y, Watanabe Y, Kumagai Y, Suematsu M,
337 Motohashi H, Fujii S, Matsunaga T. Reactive cysteine persulfides and
338 S-polythiolation regulate oxidative stress and redox signaling. *Proc. Natl. Acad.*
339 *Sci* 2014;111:7606-7611.
- 340 [32] Yu FB, Han XY, Chen LX. Fluorescent probes for hydrogen sulfide detection and
341 bioimaging. *Chem. Commun* 2014;50:12234-12249.
- 342 [33] Tang LJ, Xu D, Tian MY, Yan XM. A mitochondria-targetable far-red emissive
343 fluorescence probe for highly selective detection of cysteine with a large Stokes
344 shift. *J Lumin* 2019;208:502-508.
- 345 [34] Montoya LA, Pluth MD. Selective turn-on fluorescent probes for imaging
346 hydrogen sulfide in living cells. *Chem. Commun* 2012;48:4767-4769.
- 347 [35] Tang LJ, Tian MY, Chen HB, Yan XM, Zhong KL, Bian YJ. An ESIPT-based
348 mitochondria-targeted ratiometric and NIR-emitting fluorescent probe for
349 hydrogen peroxide and its bioimaging in living cells. *Dyes Pigments*
350 2018;158:482-489.
- 351 [36] Chen BF, Li W, Lv C, Zhao MM, Jin HW, Jin HF, Du JB, Zhang LR, Tang XJ.
352 Fluorescent probe for highly selective and sensitive detection of hydrogen sulfide
353 in living cells and cardiac tissues. *Analyst* 2013;138:946-951.
- 354 [37] Wu SZ, Li Z, Yang L, Han JH, Han SF. Fluorogenic detection of hydrogen sulfide
355 via reductive unmasking of o-azidomethylbenzoyl-coumarin conjugate. *Chem.*
356 *Commun* 2012;48:10120-10122.

- 357 [38] Bae SK, Cho BR, Kim HM. A ratiometric two-photon fluorescent probe reveals
358 reduction in mitochondrial H₂S production in parkinson's disease gene knockout
359 astrocytes. *J. Am. Chem. Soc* 2013;135:9915-9923.
- 360 [39] Velusamy N, Binoy A, Bobba KN, Nedungadi D, Bhuniya NMS. A bioorthogonal
361 fluorescent probe for mitochondrial hydrogen sulfide: new strategy for cancer cell
362 labeling. *Chem. Commun* 2017;53:8802-8805.
- 363 [40] Wang R, Yu FB, Chen LX, Chen H, Wang LJ, Zhang WW. A highly selective
364 turn-on near-infrared fluorescent probe for hydrogen sulfide detection and
365 imaging in living cells. *Chem. Commun* 2012;48:11757-11759.
- 366 [41] Liu TY, Xu ZC, Spring DR, Cui JN. Alysosome-targetable fluorescent probe for
367 imaging hydrogen sulfide in living cells. *Org. Lett* 2013;9:2310-2313.
- 368 [42] Fridkin M, Hazum E, Tauber-Finkelstein M, Shaltiel S. Thiolytic of
369 o-2,4-dinitrophenyltyrosines: Spectrophotometric monitoring of the reaction and
370 its use in peptide synthesis. *Arch. Biochem. Biophys* 1977;178:517-526.
- 371 [43] Cao XW, Lin WY, Zheng KB, He LW. A near-infrared fluorescent turn-on probe
372 for fluorescence imaging of hydrogen sulfide in living cells based on thiolysis of
373 dinitrophenyl ether. *Chem. Commun* 2012;48:10529-10531.
- 374 [44] Chalmers S, Caldwell ST, Quin C, Prime TA, James AM, Cairns AG, Murphy
375 MP, McCarron JG, Hartley RC. Selective uncoupling of individual mitochondria
376 within a cell using a mitochondria-targeted photoactivated protonophore. *J. Am.*
377 *Chem. Soc* 2012;134:758-761.

- 378 [45] Liu HY, Zhao M, Qiao QL, Lang HJ, Xu JZ, Xu ZC. Fluorescein-derived
379 fluorescent probe for cellular hydrogen sulfide imaging. *Chinese Chem. Lett*
380 2014;25:1060-1064.
- 381 [46] Yuan L, Zuo QP. FRET-based mitochondria-targetable dual-excitation ratiometric
382 fluorescent probe for monitoring hydrogen sulfide in living cells. *Chem- Asian J*
383 2014;6:1544-1549.
- 384 [47] Du ZB, Song B, Zhang WZ, Duan CC, Wang YL, Liu CL, Zhang R, Yuan JL.
385 Quantitative monitoring and visualization of hydrogen sulfide in vivo using a
386 luminescent probe based on a ruthenium(II) complex. *Angew. Chem. Int. Ed*
387 2018;57:3999-4004.
- 388 [48] Yang Y, Feng Y, Qiu FZ, Iqbal K, Wang YZ, Song XR, Wang Y, Zhang GL, Liu
389 WS. Dual-Site and Dual-Excitation Fluorescent Probe That Can Be Tuned for
390 Discriminative Detection of Cysteine, Homocysteine, and Thiophenols. *Anal.*
391 *Chem* 2018;90:14048-14055.
- 392 [49] Ren XT, Wang F, Lv J, Wei TW, Zhang W, Wang Y, Chen XQ. An ESIPT-based
393 fluorescent probe for highly selective detection of glutathione in aqueous solution
394 and living cells. *Dyes Pigments* 2016;129:156-162.
- 395 [50] Huang YY, Bae SA, Zhu ZH, Guo NN, Roth BL, Laruelle M. Fluorinated Diaryl
396 Sulfides as Serotonin Transporter Ligands: Synthesis, Structure-Activity
397 Relationship Study, and in Vivo Evaluation of Fl: 2559-2570.
- 398 [51] Chen W, Rosser EW, Matsunaga T, Pacheco A, Akaike T, Xian M. The

399 development of fluorescent probes for visualizing intracellular hydrogen
400 polysulfides. *Angew. Chem. Int. Ed* 2015;54:13961-13965.

401

402

403

404

405

406

407

408

409

410

411

412

413

414

415

416

417

418 **Figure captions**419 **Scheme 1** Synthesis of **Probe 1**.420 **Figure 1** UV-vis responses of **Probe 1** (25 μM) in DMSO : PBS (v/v, 7 : 3, pH = 7.4)
421 solution, added HS^- (0-300 μM).422 **Figure 2** (a) fluorescent responses of **Probe 1** (5 μM) toward HS^- ; Inset: Visual
423 fluorescence change photograph for **Probe 1** only and upon addition of NaHS under
424 illumination with a 365 nm UV lamp; (b) the selective of **Probe 1** (5 μM) towards HS^-
425 and various relevant analyte (100 eq.), $\lambda_{\text{ex}} = 512 \text{ nm}$, slit: 5 nm/5 nm.426 **Figure 3** (a) The working curve of **Probe 1** (5 μM) in the presence of various
427 concentrations of HS^- (0-70 μM); (b) Time dependent of **Probe 1** (5 μM) to HS^- (10
428 eq.). $\lambda_{\text{ex}} = 512 \text{ nm}$, slit: 5 nm/5 nm.429 **Scheme 2** The mechanism of the **Probe 1** responding to HS^- .430 **Figure 4** Confocal fluorescence imaging the H_2S in HepG2 cells of **Probe 1** 20 min:
431 (a1-a3) Incubated with the **Probe 1** only: (a1) green channel; (a2) brightfield image;
432 (a3) Overlay. (b1-b3) Incubated with the **Probe 1** 20 min, then treat with HS^- 20 min:
433 (b1) green channel; (b2) brightfield image; (b3) Overlay. Excitation at 488 nm, the
434 green channel was set at $545 \pm 15 \text{ nm}$ scale bar = 20 μm .435 **Figure 5**. Confocal fluorescence imaging the endogenously generated H_2S in HepG2
436 cells of **Probe 1**: (c1-c3) Incubated with the **Probe 1** only: (c1) green channel; (c2)
437 brightfield image; (c3) Overlay. (d1-d3) Incubated with the SNP for 1 h, and then
438 incubated with **Probe 1** for 20 min: (d1) green channel; (d2) brightfield image; (d3)
439 Overlay. Excitation at 488 nm, the green channel was set at $545 \pm 15 \text{ nm}$, scale bar =

440 20 μm .

441 **Figure 6.** CLSM images of Ca^{2+} regulated H_2S production pathways. (e1-e3)

442 Incubated with the **Probe 1** only: (e1) green channel; (e2) brightfield image; (e3)

443 Overlay. (f1-f3) Incubated with CaCl_2 (200 μM , 1 h), then incubated with **Probe 1** 20

444 min: (f1) green channel; (f2) brightfield image; (f3) Overlay. (g1-g3) pre-incubated

445 with AOAA (100 μM , 3 h), incubated with CaCl_2 (200 μM , 1 h), then incubated with

446 **Probe 1** 20 min: (g1) green channel; (g2) brightfield image; (g3) Overlay. (h1-h3)

447 pre-incubated with PAG (100 μM , 3 h), incubated with CaCl_2 (200 μM , 1 h), then

448 incubated with **Probe 1** 20 min: (h1) green channel; (h2) brightfield image; (h3)

449 Overlay. Excitation at 488 nm, the green channel was set at 545 ± 15 nm scale bar =

450 20 μm .

451 **Figure 7.** The *in vivo* imaging of H_2S in a nude mice model of **Probe 1** (20 μM). (a)

452 Control group; (b, c, d) First injected 40 μM **Probe 1** solution, then injected 50 μM

453 HS^- solution for 5, 10, 15 min. Excitation at 475 nm, the green channel was collected

454 at 520 ± 5 nm.

455

456

457

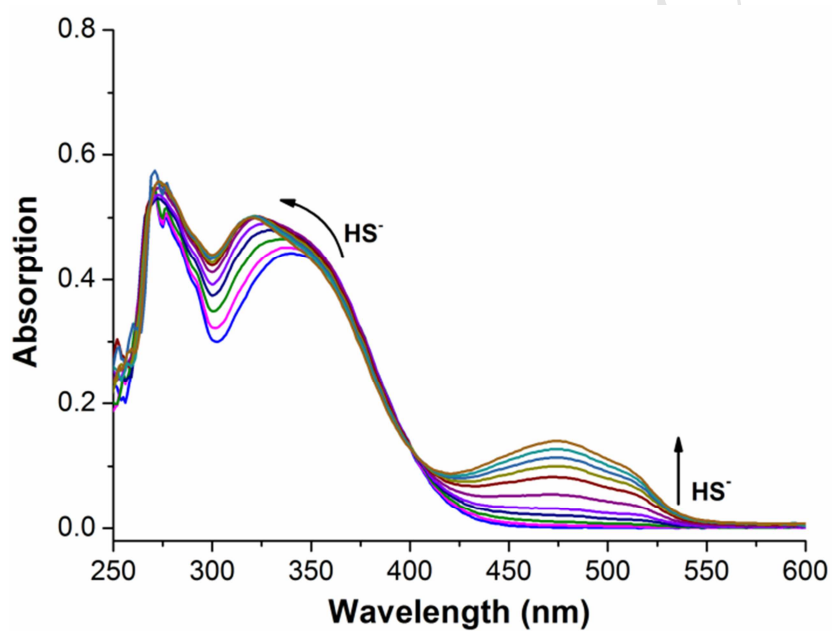
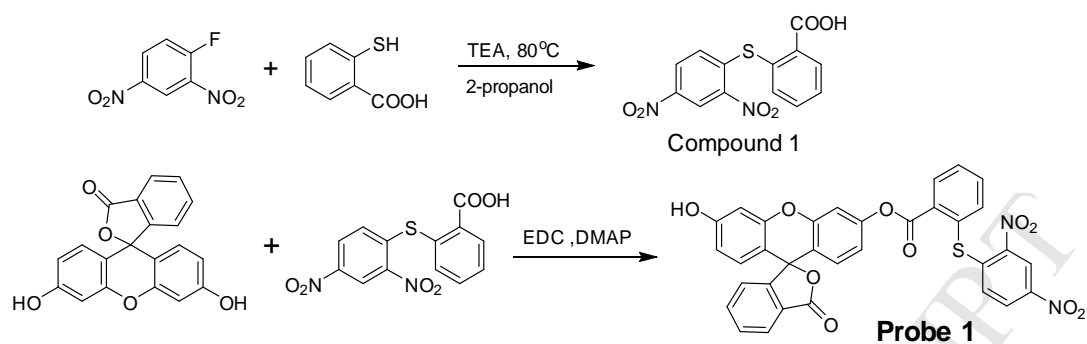
458

459

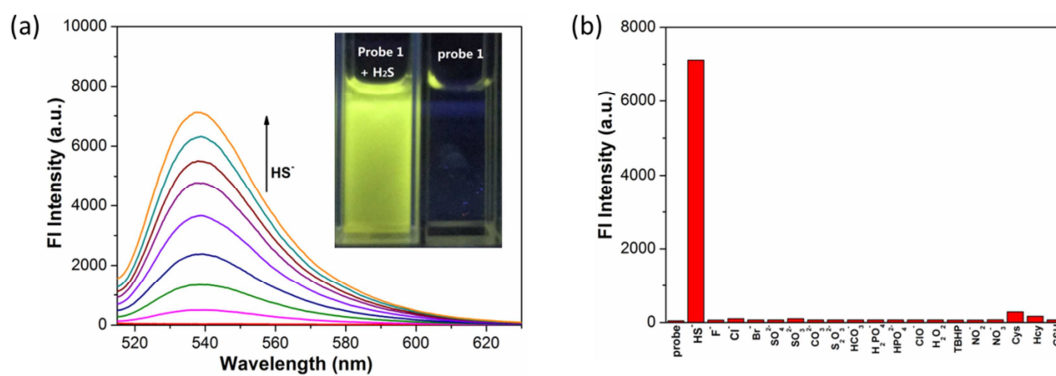
460

461

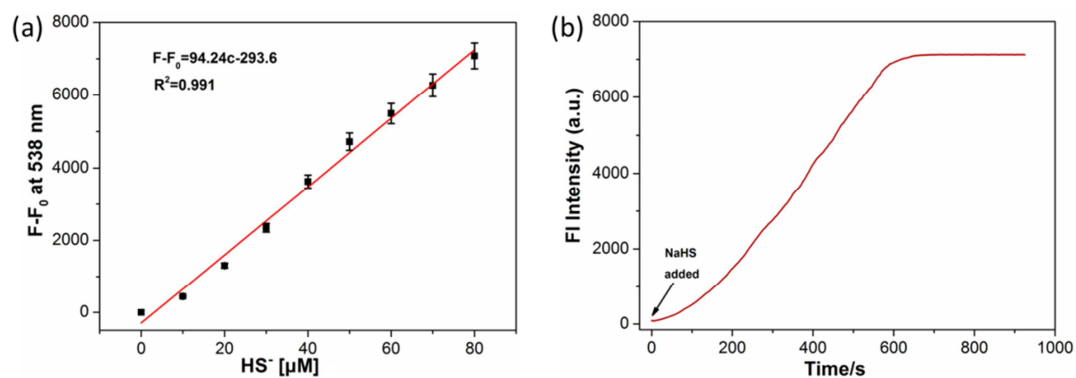
462 Scheme 1



467 Figure 2



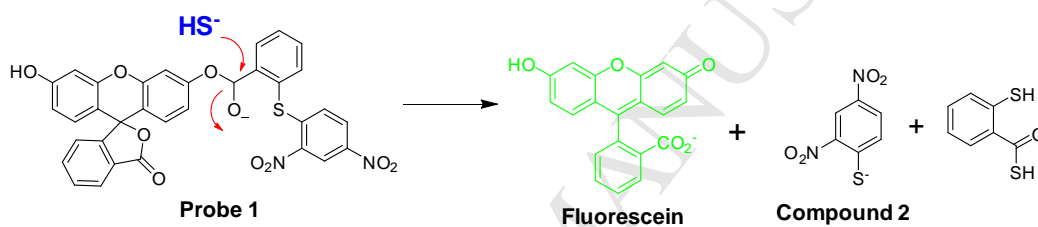
470 Figure 3



471

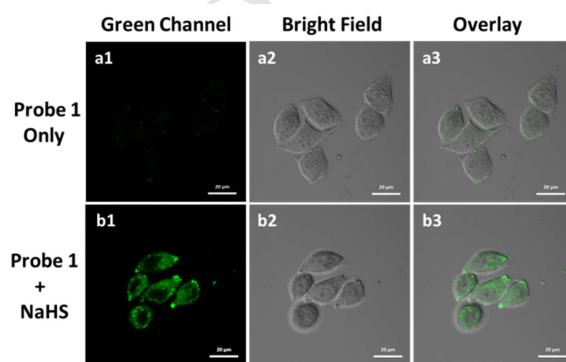
472

473 Scheme 2



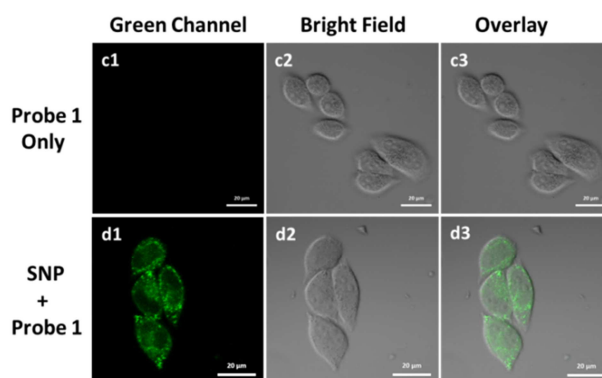
474

475 Figure 4



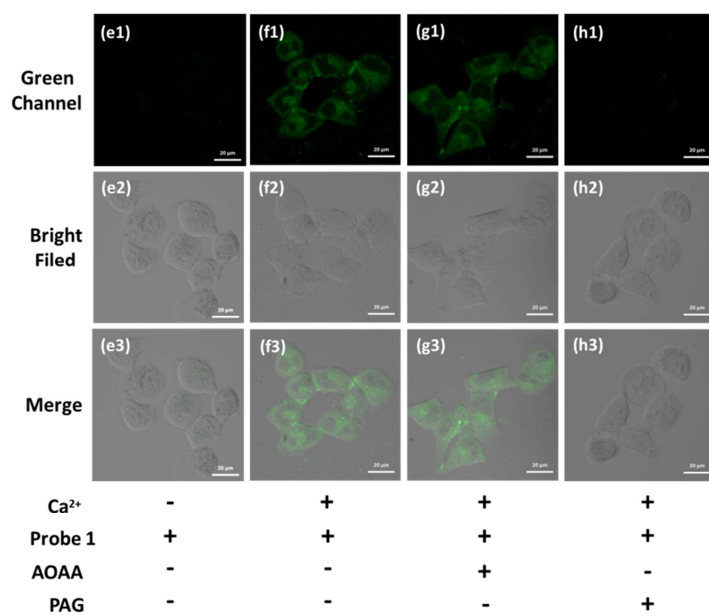
476

477 Figure 5



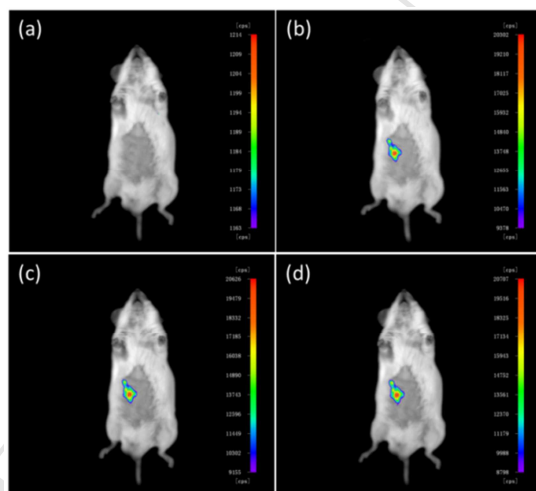
478

479 Figure 6



480

481 Figure 7



482

483

484

485

486

487

488

489

490

491

492

493

Supporting Information

494

495 **Table S1:** Compare of reported fluorescent hydrogen sulfide probes in
496 recent years.

497 **I** Material and Methods

498 **II (Fig.S1-S5):** Copies of NMR and ESI-MS of related compounds.

499 **III(Fig. S6-S9):** Spectroscopic studies.

500

501

502

503

504

505

506

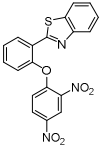
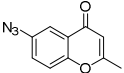
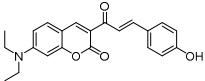
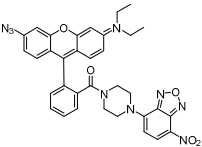
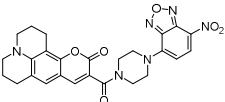
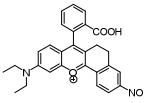
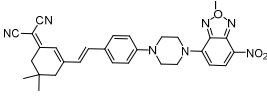
507

508

509

510 Table S1:

511 Properties of the reported fluorescent hydrogen sulfide probes in recent years.

probes	S/B ratio	detection limit	response time	Ref.
	60	10.5 nM	2.5 min	[1]
	--	18 nM	30 min	[2]
	--	50 nM	<1 min	[3]
	40	120 nM	15 min	[4]
	200	90 nM	15 min	[5]
	--	29 nM	5 min	[6]
	--	30 nM	60 min	[7]
This work (probe 1)	197	64 nM	10 min	

512 [1] Lin L, Zeng XQ, Shen YN, Zhu HL, Qian Y. An ultrasensitive fluorescent probe for rapid

513 determination of thiophenols. *Talanta* 2017;165:321-325.

514 [2] Qiao Z, Zhang HY, Wang KW, Zhang YR. A highly sensitive and responsive fluorescent probe

515 based on 6-azidechroman dye for detection and imaging of hydrogen sulfide in cells. *Talanta*

516 2019;195:850-856.

517 [3] Yang Y, Feng Y, Jiang Y, Qiu FZ, Wang YZ, Song XR, Tang XL, Zhang GL, Liu WS. A

518 coumarin-based colorimetric fluorescent probe for rapid response and highly sensitive detection of

519 hydrogen sulfide in living cells. *Talanta* 2019;197:122-129.

520 [4] Ma C, Wei C, Li XY, Zheng XY, Chen B, Wang M, Zhang PZ, Li XL. A mitochondria-targeted
521 dual-reactable fluorescent probe for fast detection of H₂S in living cells. *Dyes and Pigments* 2019;
522 162:624-631.

523 [5] Ismail I, Wang DW, Wang ZH, Wang D, Zhang CY, Yi L, Xi Z. A julolidine-fused
524 coumarin-NBD dyad for highly selective and sensitive detection of H₂S in biological samples.
525 *Dyes and Pigments* 2019;163:700-706.

526 [6] Chen HH, Gong XY, Liu XW, Li Z, Zhang JJ, Yang XF. A nitroso-based fluorogenic probe for
527 rapid detection of hydrogen sulfide in living cells. *Sensors Actuators: B. Chemical*
528 2019;281:542-548.

529 [7] Huang XT, Liu HY, Zhang JW, Xiao BR, Wu FX, Zhang YY, Tan Y, Jiang YY. A novel
530 near-infrared fluorescent hydrogen sulfide probe for live cell and tissue imaging. *New J. Chem.*,
531 2019;43:6848-6855.

532

533 **I. Materials and apparatus.**

534 Reagents with analytical grades were purchased from commercial and used without
535 further purification.

536 UV-vis spectra were taken on a HITACHI U-3900 spectrophotometer and
537 fluorescence spectra were recorded using a HITACHI F-7000 spectrophotometer. ¹H
538 NMR and ¹³C NMR experiments were measured by a Bruker AVANCE-600 MHz
539 spectrometer (Bruker, Billerica, MA). Electrospray ionization (ESI) mass spectra were

540 acquired using an AB Triple TOF 5600plus System (AB SCIEX, Framingham, USA).

541 The cell imaging experiments used Zeiss LSM880 CLSM.

542

543 *Imaging Experiments*

544 HepG2 cells and HeLa cells were cultured in dulbecco's modified eagle's medium
545 (DMEM, Gibco) in an atmosphere of 5% CO₂ and 95% air at 37 °C. Before the
546 CLSM imaging, the cells were plated on 14 mm glass coverslips and were incubated
547 overnight. The cells were washed with PBS and then incubated with **Probe 1** in
548 DMSO/PBS (0.5 %, v/v) for 3 h at 37 °C. After washing three times, the cells were
549 subjected to CLSM imaging.

550 Imaging procedures were conducted with adult nude mice under general anesthesia
551 by injection of sodium pentobarbital (0.5 mL/0.03%). Images were taken using an
552 excitation of 475 nm and emission was collected 520±5 nm.

553

554

555

556

557

558

559

560

561

562

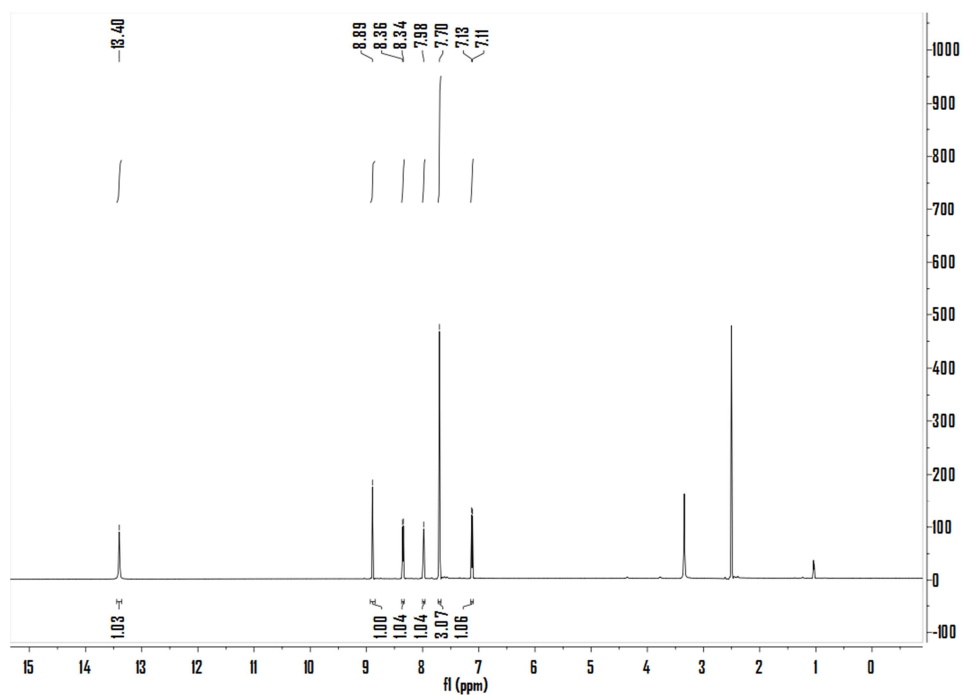
563

564

565 II : Copies of NMR and ESI-MS of related compounds

566 Fig. S1

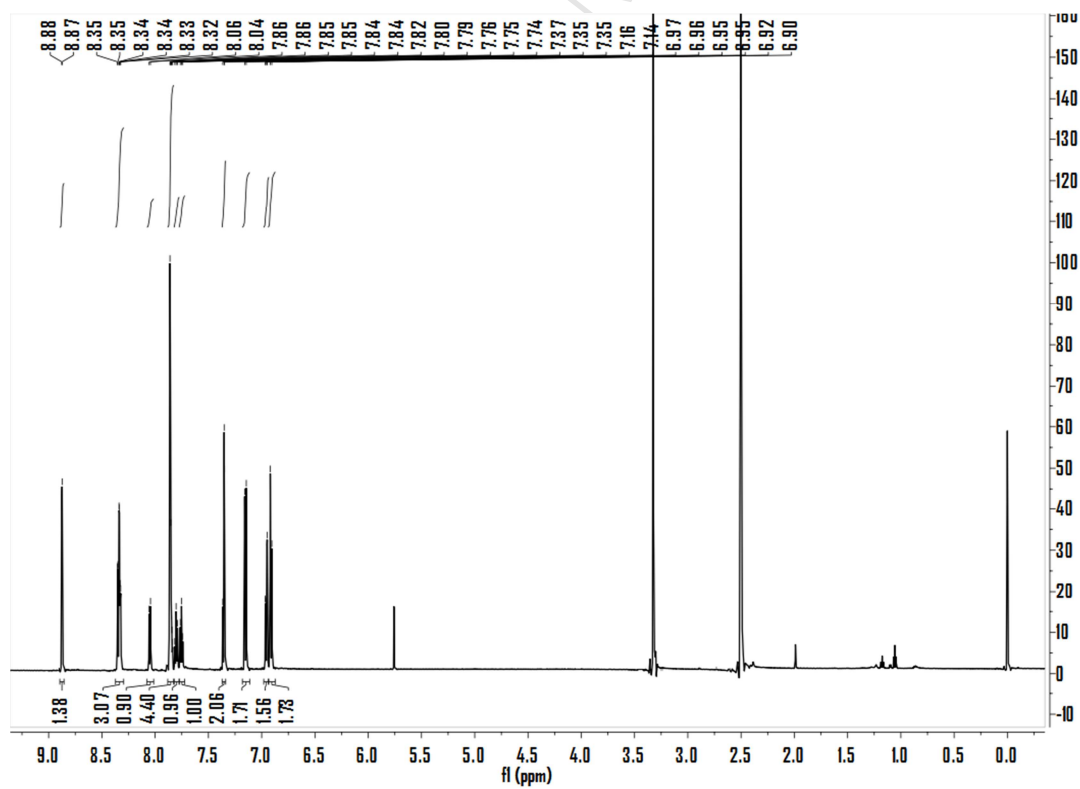
567



568

569 Figure S1. The ^1H NMR (600 MHz) spectra of the compound 1 in $\text{DMSO-}d_6$.

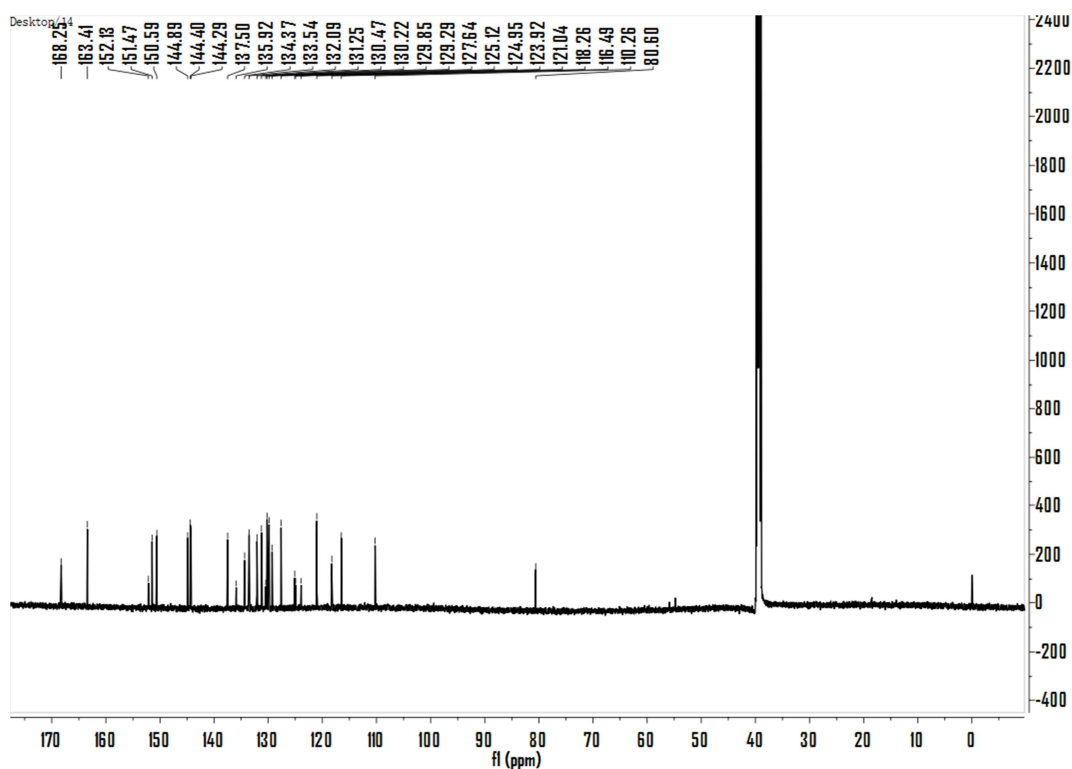
570



571

572 Figure S2. The ^1H NMR (600 MHz) spectra of the **Probe 1** in $\text{DMSO-}d_6$.

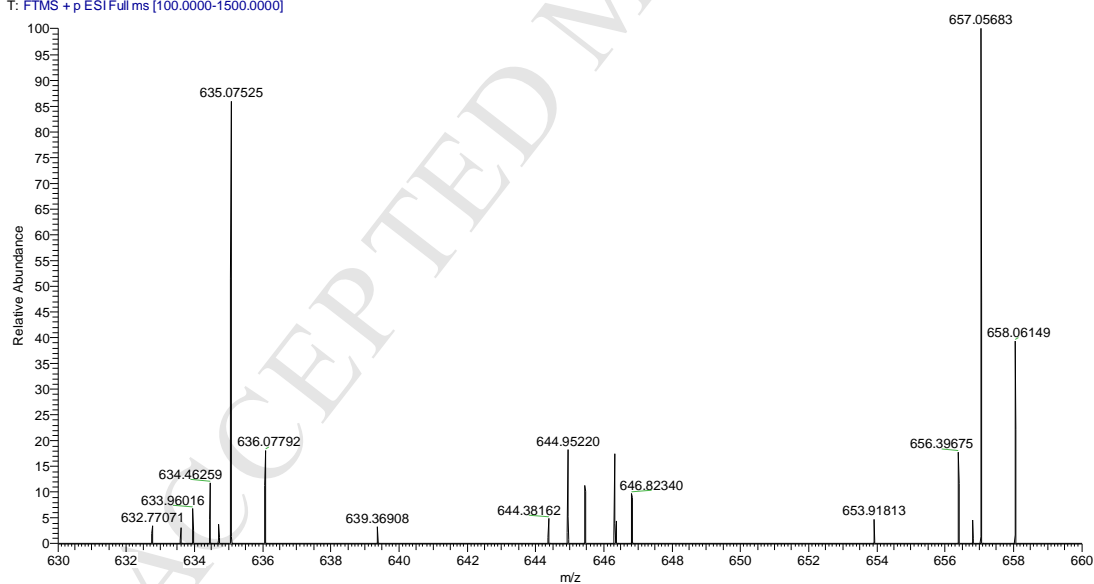
573 Fig. S3



574

575 Figure S3. The ^{13}C NMR (150 MHz) spectra of the **Probe 1** in $\text{DMSO-}d_6$.576 **Fig. S4**

KJ509-1 #16-20 RT: 0.16-0.18 AV: 2 NL: 3.02E6
T: FTMS + p ESI Full ms [100.0000-1500.0000]

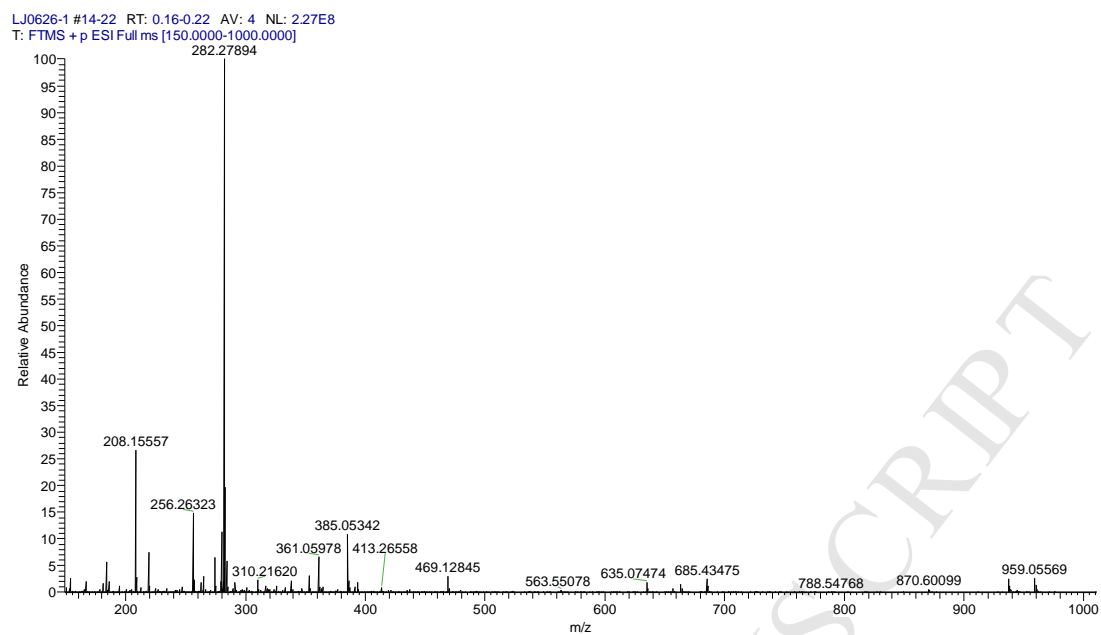


577

578 Figure S4: ESI-MS of the **Probe 1**: [**Probe 1** + H]⁺ Calcd for 635.076, Found 635.076; [**probe 1** + Na]⁺ Calcd for
579 657.058, Found 657.057.

580 **Fig. S5**

581

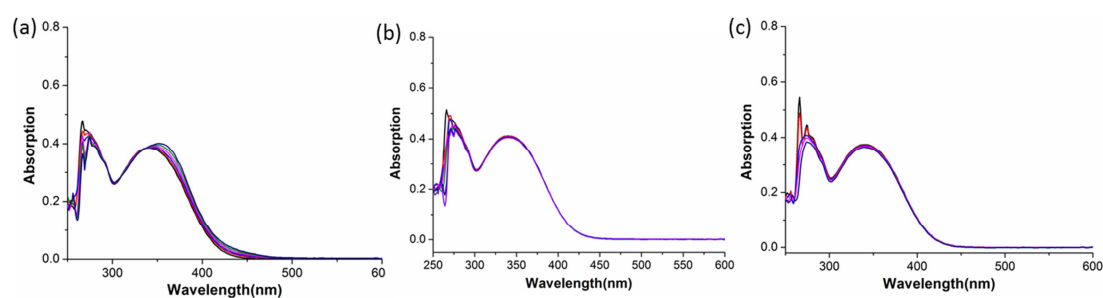


582

583 Figure S5: ESI-MS of the complete whole m/z range of the **Probe 1**: [**Probe 1** + H]⁺ Calcd for 635.076, Found
584 635.076.

585 III. Spectroscopic Studies

586 Fig. S6



587

588 Figure S7. In 2 mL DMSO : PBS (v/v, 7 : 3, pH = 7.4) solution of **Probe 1** (25 μ M), added of 500
589 μ M (a) Cys; (b) Hcy; (c) GSH.

590

591

592

593

594

595

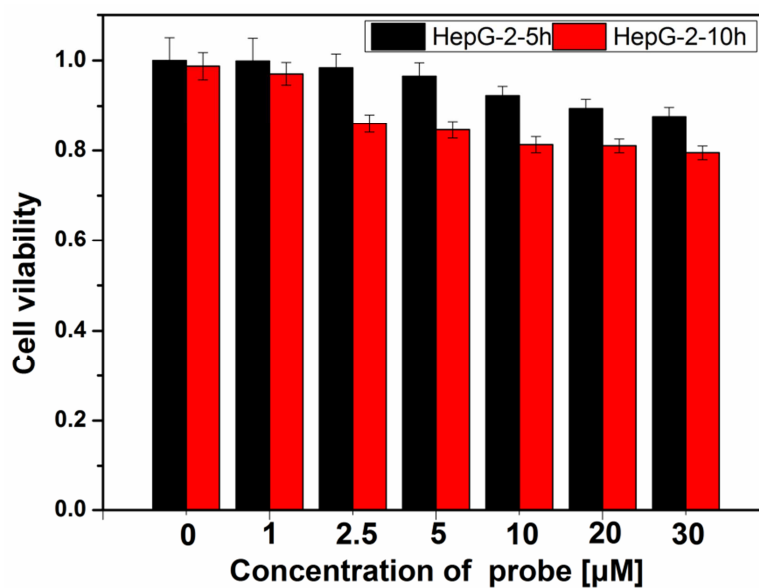
596

597

598

599

600

601 **Fig. S8**

602

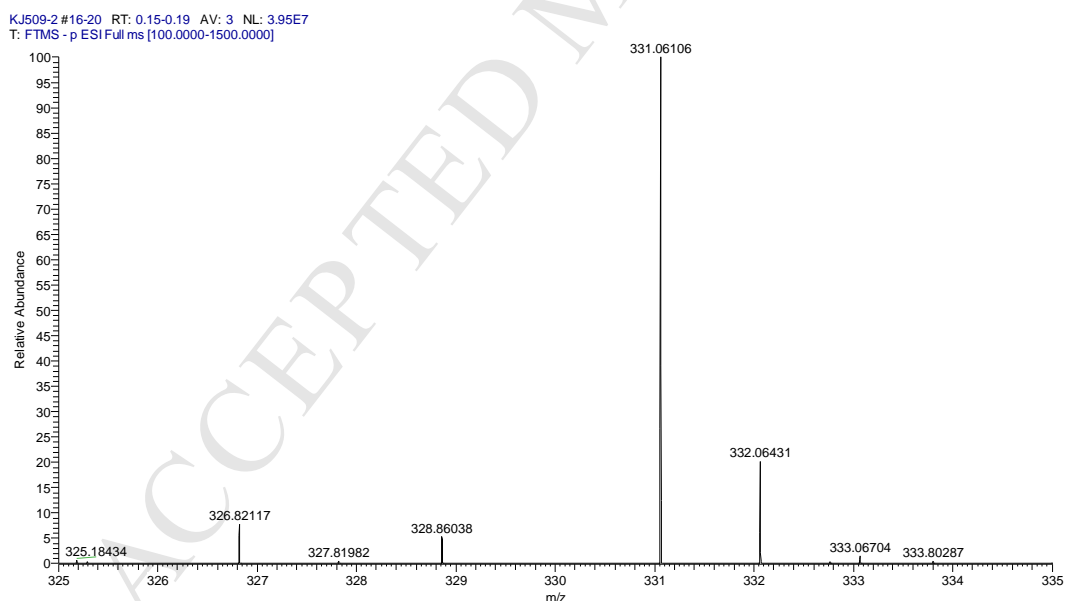
603 Figure S8. Cytotoxicity of **Probe 1** toward HepG2 cells.

604

605

606 **Fig. S9**

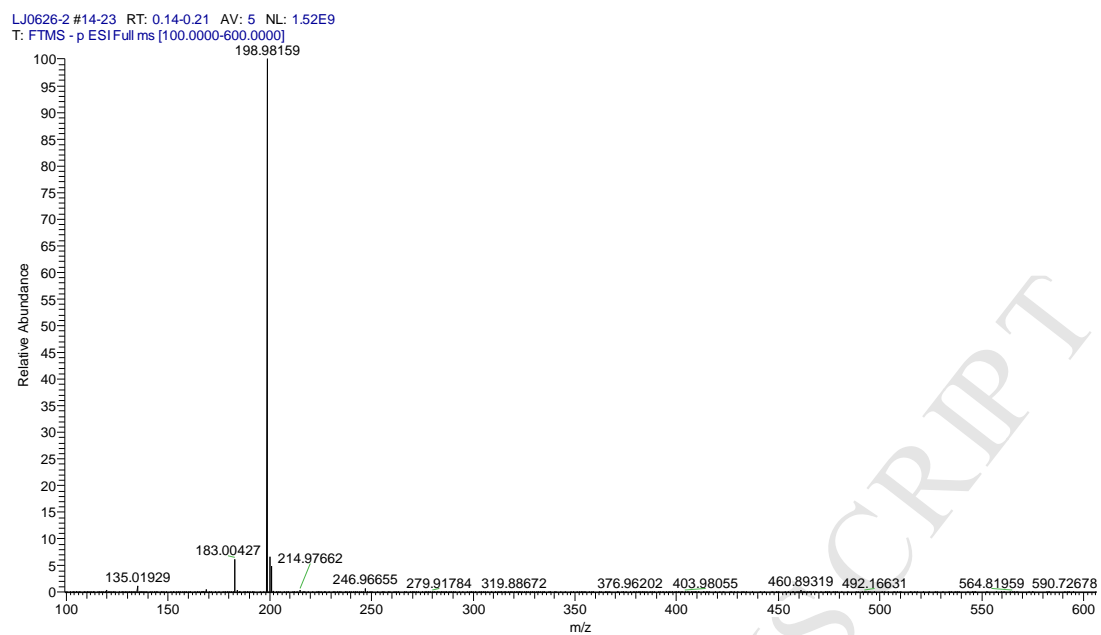
607



608

609

610



611

612

613 Figure S9. ESI-MS of a solution mixture of **Probe 1** and NaHS exhibited dominant m/z peaks at
614 331.06, 198.98, 168.95 in accordance with the fluorescein: 331.06, compound 2: 198.98.

615

616

617